Computational Materials Science 48 (2010) 736–742

Contents lists available at ScienceDirect

Computational Materials Science

journal homepage: www.elsevier.com/locate/commatsci

Torsional buckling of carbon nanotubes based on nonlocal elasticity shell models

F. Khademolhosseini [a], R.K.N.D. Rajapakse [b,*], A. Nojeh [c]

[a] Department of Mechanical Engineering, University of British Columbia, Vancouver, Canada V6T 1Z4
[b] Faculty of Applied Sciences, Simon Fraser University, Burnaby, Canada V5A 1S6
[c] Department of Electrical and Computer Engineering, University of British Columbia, Vancouver, Canada V6T 1Z4

ARTICLE INFO

Article history:
Received 17 January 2010
Received in revised form 26 February 2010
Accepted 15 March 2010
Available online 14 April 2010

Keywords:
Carbon nanotubes
Torsion
Buckling
Nonlocal elasticity
Molecular dynamics
Shells

ABSTRACT

This paper investigates size-effects in the torsional response of single walled carbon nanotubes (SWCNTs) by developing a modified nonlocal continuum shell model. The purpose is to facilitate the design of devices based on SWCNT torsion by providing a simple, accurate and efficient continuum model that can predict the corresponding buckling loads. To this end, Eringen's equations of nonlocal elasticity are incorporated into the classical models for torsion of cylindrical shells given by Timoshenko and Donnell. In contrast to the classical models, the nonlocal model developed here predicts non-dimensional buckling torques that depend on the values of certain geometric parameters of the CNT, allowing for the inclusion of size-effects. Molecular dynamics simulations of torsional buckling are also performed and the results of which are compared with the classical and nonlocal models and used to extract consistent values of shell thickness and the nonlocal elasticity constant (e_0). A thickness of 0.85 Å and nonlocal constant values of approximately 0.8 and 0.6 for armchair and zigzag nanotubes respectively are recommended for torsional analysis of SWCNTs using nonlocal shell models. The size-dependent nonlocal models together with molecular dynamics simulations show that classical shell models overestimate the critical buckling torque of SWCNTs and are not suitable for modeling of SWCNTs with diameters smaller than 1.5 nm.

1. Introduction

Carbon nanotubes (CNTs) have attracted much attention because of their superior mechanical, optical, thermal and electrical properties and potential applications in the development of novel nano-scale devices [1–3]. Further development of CNT-based devices requires a good understanding of their mechanical behavior. Basic mechanical properties such as Young's modulus, shear modulus, Poisson's ratio and maximum tensile and compressive strengths have been studied rigorously, a review of which is given by Qian et al. [4]. Different approaches have been used to characterize CNT properties; first-principles methods based on quantum mechanical calculations, semi-empirical methods such as molecular dynamics (MD) simulations, continuum modeling and experimental methods which mostly consist of CNT manipulation with Atomic Force Microscopes [5–7]. Of these, first-principles methods are the most accurate, but are computationally expensive and limited to the study of systems with a small number of atoms.

Continuum modeling is perhaps the most computationally efficient method for the theoretical study of CNTs, but classical continuum models are unable to account for quantum effects arising from the discrete nature of matter at the nano-scale. To overcome this issue, modified continuum models have been proposed which can deal with larger systems but are also able to include nano-scale size-effects. Multi-scale continuum models [8], surface energy incorporated models [9] and nonlocal elasticity [10–13] have been successfully used to this end.

An important issue in the CNT continuum modeling is the selection of appropriate values for the continuum properties such as the equivalent elastic modulus and CNT thickness [14,15]. It is challenging to determine these quantities in a consistent manner and there are discrepancies in the values reported in the literature. One possible solution is the atomisitc-based finite deformation shell theory proposed by Wu et al. [15] where the constitutive relations between stress, moment and strain are given in terms of inter-atomic potentials without the need to define a value for shell thickness. This theory has been used to study tension, torsion and bending of CNTs [15].

Recently, a number of nano-scale devices have been developed which use carbon nanotubes as torsional elements [16–18]. Therefore, it is important to fully understand the torsional properties of CNTs such as the buckling strain and buckling torque for reliable design of nano-scale torsional devices.

Wang and Wang [19] used a classical multi-shell model to study the torsional buckling of multi-walled carbon nanotubes (MWCNTs). Lu and Wang [20] studied the torsional buckling of MWCNTs under combined torque and axial loads using a classical

* Corresponding author.
E-mail address: rajapakse@sfu.ca (R.K.N.D. Rajapakse).

0927-0256/$ - see front matter © 2010 Elsevier B.V. All rights reserved.
doi:10.1016/j.commatsci.2010.03.021

shell model. Wang et al. [21] studied the torsional buckling of CNTs using classical shell models and determined the applicability of different models for a range of CNTs with different aspect ratios. The aforementioned continuum models are based on the classical elasticity theory [22] and are unable to capture the size-dependency of CNT structural response, which could result in inaccurate estimation of the critical loads.

In this paper, an isotropic continuum shell model for the torsion of CNTs based on the concepts of nonlocal elasticity [10] is proposed to account for the size-dependency. The objective is to study size-effects on the torsional buckling of carbon nanotubes which is a determining factor for the design of torsion based CNT devices. It is also shown that the nonlocal elasticity parameter can be determined from molecular dynamic simulations through a non-linear optimization process, and that classical elastic shell models are unable to predict the torsional buckling loads that match well with molecular dynamics results. It is seen that the modified nonlocal model presented here, along with the values for shell thickness and nonlocal constant extracted from MD simulations can be used to efficiently and accurately predict the buckling torque of CNTs, a necessary step in the design of devices based on CNT torsion.

2. Modified continuum shell model based on nonlocal elasticity

The concept of nonlocal elasticity was first introduced by Eringen [10] in the 1980s to study screw dislocation and surface waves in solids. Unlike classical elasticity models, the nonlocal elasticity theory assumes that the stress at a reference point X in a body depends not only on the strains at X, but also on strains at all other points of the body [10]. Peddison et al. [11] recently studied the bending of nano-scale beams using nonlocal elasticity and concluded that size-effects could be significant for nano-sized structures. Zhang et al. [12,13] used nonlocal elasticity to show the small-scale effects on buckling of MWCNTs under axial compression and radial pressure. A number of other researchers have used nonlocal elasticity to study the vibration and propagation of waves in CNTs [23,24].

It is important to note the fact that a graphene sheet is an isotropic structure. An apparent anisotropy (directional dependence of modulus) is introduced when a graphene sheet is rolled up to produce a tube. The root of anisotropy of a nanotube is therefore related to chirality (roll up vector) in contrast to inherent material anisotropy. A nanotube can therefore be represented by an 'equivalent' isotropic material with a modulus that is a function of chirality. In our opinion, it is unnecessary to use traditional anisotropy models involving several elastic moduli as it would be difficult to physically determine these moduli.

In the ensuing sections, two new nonlocal elastic isotropic thin shell models for the torsional buckling of CNTs are proposed. These models are obtained by modifying the classical Timoshenko model [22] and the Donnell model [25] by using the concepts of nonlocal theory of elasticity [10]. It is assumed that a CNT can be represented by an isotropic cylindrical thin shell with an average diameter equal to that of the nanotube.

2.1. Modified Timoshenko shell model

Fig. 1 shows the geometry of a cylindrical shell of radius a with a cylindrical coordinate system (r, θ, x) with the x-axis along centre of the cylinder.

The displacements in the axial, circumferential and radial directions, measured from the twisted equilibrium state of the shell are denoted by u, v and w respectively and are functions of only x and θ. The non-zero strains ε_{xx}, $\varepsilon_{x\theta}$ and $\varepsilon_{\theta\theta}$ can be expressed in terms of displacements in their classical sense [22].

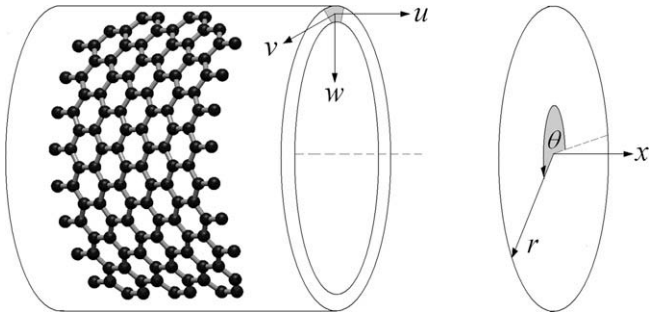

Fig. 1. Cylindrical thin shell representation of a SWCNT with the coordinate system.

Following Eringen [10], the nonlocal elasticity based stress–strain relationship which relates the non-zero stresses σ_{xx}, $\sigma_{x\theta}$ and $\sigma_{\theta\theta}$ to the non-zero strains of the present class of problems can be expressed in the following form:

$$\begin{aligned}
\sigma_{xx} - \xi\nabla_R^2\sigma_{xx} &= \frac{E}{1-\upsilon^2}(\varepsilon_{xx} + \upsilon\varepsilon_{\theta\theta}) \\
\sigma_{\theta\theta} - \xi\nabla_R^2\sigma_{\theta\theta} &= \frac{E}{1-\upsilon^2}(\varepsilon_{\theta\theta} + \upsilon\varepsilon_{xx}) \\
\sigma_{x\theta} - \xi\nabla_R^2\sigma_{x\theta} &= \frac{E}{1+\upsilon}\varepsilon_{x\theta}
\end{aligned} \tag{1}$$

where $\nabla_R^2 = \frac{\partial^2}{\partial x^2} + \frac{1}{a^2}\frac{\partial^2}{\partial\theta^2}$, $\xi = (e_0 d)^2$; e_0 is the nonlocal constant for a given material; d is an internal characteristic length of a material, i.e., the inter-atomic distance; and E and υ are Young's modulus and Poisson's ratio respectively.

Substitution of classical strain–displacement relations in (1) and integration over a cross-sectional element of unit width yields,

$$\begin{aligned}
N_{xx} - \xi\nabla_R^2 N_{xx} &= \frac{Eh}{1-\upsilon^2}\left(\frac{\partial u}{\partial x} + \upsilon\left(\frac{1}{a}\frac{\partial v}{\partial\theta} - \frac{w}{a}\right)\right) \\
N_{\theta\theta} - \xi\nabla_R^2 N_{\theta\theta} &= \frac{Eh}{1-\upsilon^2}\left(\frac{1}{a}\frac{\partial v}{\partial\theta} - \frac{w}{a} + \upsilon\frac{\partial u}{\partial x}\right) \\
N_{x\theta} - \xi\nabla_R^2 N_{x\theta} &= \frac{Eh}{2(1+\upsilon)}\left(\frac{1}{a}\frac{\partial u}{\partial\theta} + \frac{\partial v}{\partial x}\right)
\end{aligned} \tag{2}$$

$$\begin{aligned}
M_{xx} - \xi\nabla_R^2 M_{xx} &= -\frac{Eh^3}{12a(1-\upsilon^2)}\left(\frac{\partial^2 w}{\partial x^2} + \frac{\upsilon}{a^2}\left(\frac{\partial^2 w}{\partial\theta^2} + \frac{\partial v}{\partial\theta}\right)\right) \\
M_{\theta\theta} - \xi\nabla_R^2 M_{\theta\theta} &= -\frac{Eh^3}{12a(1-\upsilon^2)}\left(\upsilon\frac{\partial^2 w}{\partial x^2} + \frac{1}{a^2}\left(\frac{\partial^2 w}{\partial\theta^2} + \frac{\partial v}{\partial\theta}\right)\right) \\
M_{x\theta} - \xi\nabla_R^2 M_{x\theta} &= \frac{Eh^3}{12a(1+\upsilon)}\left(\frac{\partial v}{\partial x} + \frac{\partial^2 w}{\partial x\partial\theta}\right)
\end{aligned} \tag{3}$$

where N_{ij} $(i, j = x, \theta)$ is the force per unit length and M_{ij} $(i, j = x, \theta)$ is the moment per unit length on a cross section of the shell respectively; and h is the shell thickness (Fig. 2).

Substituting Eqs. (2) and (3) into the classical equations of translational and rotational equilibrium for a cylindrical shell prior

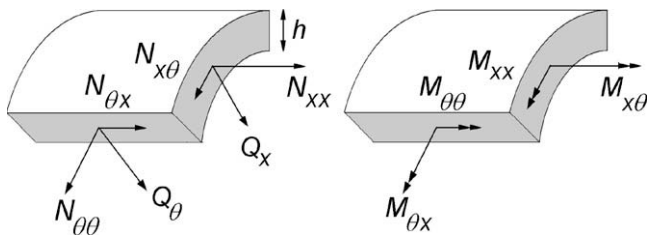

Fig. 2. Definition of forces and moments per unit length acting on a shell.

to buckling [22], the following system of coupled differential equations are obtained for the displacements u, v and w.

$$a^2\frac{\partial^2 u}{\partial x^2}+\frac{1}{2}(1-\upsilon)\frac{\partial^2 u}{\partial\theta^2}+\frac{1}{2}a(1+\upsilon)\frac{\partial^2 v}{\partial x\partial\theta}-\upsilon a\frac{\partial w}{\partial x}+a\phi\left(\frac{\partial^2 u}{\partial x\partial\theta}-a\frac{\partial^2 v}{\partial x^2}\right)-a\phi\xi\left(\frac{\partial^4 u}{\partial x^3\partial\theta}+\frac{1}{a^2}\frac{\partial^4 u}{\partial x\partial\theta^3}-\frac{1}{a}\frac{\partial^4 v}{\partial x^2\partial\theta^2}-a\frac{\partial^4 v}{\partial x^4}\right)=0 \quad (4\text{ - a})$$

$$\frac{\partial^2 v}{\partial\theta^2}+\frac{1}{2}a^2(1-\upsilon)\frac{\partial^2 v}{\partial x^2}+\frac{1}{2}a(1+\upsilon)\frac{\partial^2 u}{\partial x\partial\theta}-\frac{\partial w}{\partial\theta}+\alpha\left(\frac{\partial^2 v}{\partial\theta^2}+a^2(1-\upsilon)\frac{\partial^2 v}{\partial x^2}+a^2\frac{\partial^3 w}{\partial x^2\partial\theta}+\frac{\partial^3 w}{\partial\theta^3}\right)+2a\phi\left(\frac{\partial^2 v}{\partial x\partial\theta}-\frac{\partial w}{\partial x}\right)-2a\phi\xi\left(\frac{\partial^4 v}{\partial x^3\partial\theta}+\frac{1}{a^2}\frac{\partial^4 v}{\partial x\partial\theta^3}-\frac{1}{a^2}\frac{\partial^3 w}{\partial x\partial\theta^2}-\frac{\partial^3 w}{\partial x^3}\right)=0 \quad (4\text{ - b})$$

$$\frac{\partial v}{\partial\theta}+a\upsilon\frac{\partial u}{\partial x}-w-\alpha\left(a^4\frac{\partial^4 w}{\partial x^4}+2a^2\frac{\partial^4 w}{\partial x^2 d\theta^2}+\frac{\partial^4 w}{\partial\theta^4}-(2-\upsilon)a^2\frac{\partial^3 v}{\partial x^2 d\theta}-\frac{\partial^3 v}{\partial\theta^3}\right)+2a\phi\left(\frac{\partial^2 w}{\partial x\partial\theta}+\frac{dv}{dx}\right)-2a\phi\xi\left(\frac{\partial^3 v}{\partial x^3}+\frac{1}{a^2}\frac{\partial^3 v}{\partial x\partial\theta^2}+\frac{1}{a^2}\frac{\partial^4 w}{\partial x\partial\theta^3}+\frac{\partial^4 w}{\partial x^3\partial\theta}\right)=0 \quad (4\text{-c})$$

where $\phi=\frac{T(1-\upsilon^2)}{2\pi a^2 Eh}$, T is the applied torque prior to buckling and $\alpha=\frac{h^2}{12a^2}$.

For a long cylinder, the buckling displacements can be expressed as [22]

$$u=A\cos\left(\frac{\lambda x}{a}-n\theta\right)v=B\cos\left(\frac{\lambda x}{a}-n\theta\right)w=C\sin\left(\frac{\lambda x}{a}-n\theta\right) \quad (5)$$

where $\lambda=\frac{m\pi a}{l}$, m is number of half waves in the axial direction corresponding to an axial half-wave length of $\pi a/\lambda$ and n is the number of waves in the circumferential direction.

Substitution of Eq. (5) in (4) and the solution of the resulting eigenvalue problem, the critical buckling torque of the modified Timoshenko model based on nonlocal elasticity theory (M_{Cr}^{NT}) and its non-dimensional value ($\overline{M}_{Cr}^{NT}$) are:

$$\overline{M}_{cr}^{NT}=\frac{M_{cr}^{NT}}{E\sqrt{ah^5}}=\frac{\frac{\pi\sqrt{2}}{3(1-\upsilon^2)^{3/4}}}{1+n^2e_0^2\left(\frac{d}{a}\right)^2} \quad (6)$$

For comparison, the non-dimensional buckling torque ($\overline{M}_{Cr}^{T}$) corresponding to the classical thin shell model based on ideal elasticity is

$$\overline{M}_{cr}^{T}=\frac{M_{cr}^{T}}{E\sqrt{ah^5}}=\frac{\pi\sqrt{2}}{3(1-\upsilon^2)^{3/4}} \quad (7)$$

Therefore,

$$\frac{\overline{M}_{cr}^{T}}{\overline{M}_{cr}^{NT}}=\frac{M_{cr}^{T}}{M_{cr}^{NT}}=1+n^2e_0^2\left(\frac{d}{a}\right)^2 \quad (8)$$

The results of Eqs. (6) and (7) are based on the following critical value for λ given by Timoshenko and Gere [22];

$$\lambda_{cr}=\sqrt{\frac{2h}{a\sqrt{(1-\upsilon^2)}}} \quad (9)$$

It is clear from Eqs. (6) and (7) the former is size-dependent due to the presence of the shell radius in the denominator. From Eq. (8) it is seen that the ratio of the classical to nonlocal critical torques increases with decreasing values of the nanotube radius (a) and number of waves in the circumferential direction of the buckled shape (n). Note that when $e_0 = 0$, obviously the nonlocal model result reduces to the classical solution.

2.2. Modified Donnell shell model

Compared to Timoshenko's model [22], Donnell's shell model [25] is simpler since the governing differential equation of the system depends only on the radial displacement w. In Donnell's analysis, the radial equilibrium of the shell is considered. Substitution of Eqs. (2) and (3) into the classical equilibrium equations proposed by Donnell [25] yields the following governing equation for torsional buckling of cylindrical shells in terms of the radial displacement.

$$D\nabla_R^8 w=\frac{2}{a}N_{x\theta}^0\frac{\partial^2}{\partial x\partial\theta}\left(\nabla_R^4 w\right)-\frac{Eh}{a^2}\frac{\partial^4 w}{\partial x^4}-\xi\left(\frac{2}{a}N_{x\theta}^0\frac{\partial^2}{\partial x\partial\theta}\left(\nabla_R^6 w\right)\right) \quad (10)$$

where $D=\frac{Eh^3}{12(1-\upsilon^2)}$ is the bending rigidity and $N_{x\theta}^0$ is the shearing force at the onset of buckling. When $\xi = 0$, Eq. (10) reduces to the classical Donnell model governing equation [25]. The buckling torque is determined from Eq. (10) by assuming that the buckling mode-shape is of the following form:

$$w=A\sin\left(\frac{\lambda x}{a}-n\theta\right)\lambda=\frac{m\pi a}{l} \quad (11)$$

The solution for the shearing force $N_{x\theta}^0$ at the onset of buckling is:

$$N_{x\theta}^0=\frac{\frac{D(\lambda^2+n^2)^4}{a^2}+Eh\lambda^4}{2\lambda n(\lambda^2+n^2)^2\left(1+e_0^2\frac{d^2}{a^2}(\lambda^2+n^2)\right)} \quad (12)$$

Minimizing Eq. (12) with respect to λ and using the relation $T=2\pi a^2 N_{x\theta}^0$, the critical buckling torque of the modified Donnell model based on nonlocal elasticity theory (M_{cr}^{ND}) and its non-dimensional value ($\overline{M}_{cr}^{ND}$) are:

$$\overline{M}_{cr}^{ND}=\frac{M_{cr}^{ND}}{E\sqrt{ah^5}}=\frac{\frac{\pi\sqrt{2.3}}{3(1-\upsilon^2)}^{3/4}}{1+e_0^2\frac{d^2}{a^2}(\lambda^2+n^2)} \quad (13)$$

For comparison, the non-dimensional buckling torque of the classical Donnell model is:

$$\overline{M}_{cr}^{D}=\frac{M_{cr}^{D}}{E\sqrt{ah^5}}=\frac{\pi\sqrt{2.3}}{3(1-\upsilon^2)^{3/4}} \quad (14)$$

Therefore,

$$\frac{\overline{M}_{cr}^{D}}{\overline{M}_{cr}^{ND}}=\frac{M_{cr}^{D}}{M_{cr}^{ND}}=1+e_0^2\frac{d^2}{a^2}(\lambda^2+n^2) \quad (15)$$

It has been shown [22] that the minimum critical buckling torque corresponds to $n = 2$ and for small values of λ^2 compared to n^2 the above equation becomes identical to the ratio of critical buckling torques obtained from the Timoshenko model. Note that classical Donnell's model has a higher buckling torque compared to the classical Timoshenko model (Eq. (12)).

Fig. 3 shows the ratio of classical to modified critical buckling torques obtained from Eqs. (8)–(15) for the values of λ_{cr} calculated from Eq. (9) and a value of $d = 1.41$ Å used as the inter-atomic spacing of the CNT structure. It is seen that for CNTs with small radii, i.e., less than 0.7 nm, the classical buckling torque is significantly higher than the nonlocal buckling torque.

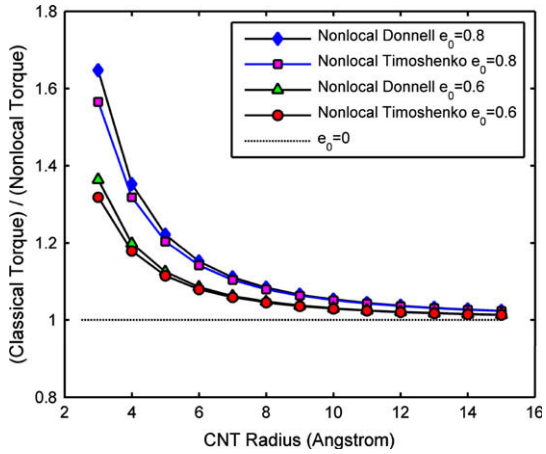

Fig. 3. Ratio of classical to nonlocal buckling torques for two different values of e_0.

3. Molecular dynamics modeling of torsional buckling

The software package Nanohive1 [26], incorporated with the AIREBO potential field [27] is used to perform molecular dynamic simulations on a range of nanotubes in order to determine the equivalent continuum properties applicable to the current continuum shell models and assess their validity in CNT modeling. The Adaptive Intermolecular Reactive Empirical Bond Order (AIREBO) potential is an extension of the commonly used REBO potential developed for solid carbon and hydrocarbon molecules [28]. The extensions that AIREBO potential provides are:

(a) Non-bonded, intermolecular interactions, modeled with a Lennard–Jones (LJ) 12-6 potential
(b) Four-body torsional interaction, modeled with a torsional potential with a single minimum

In the present simulations, once the buckling has occurred, the four-body torsional potential becomes important and can affect the equilibrium deformation of the system. To determine the buckling state of a certain nanotube under torsion, the modeling is started from an initial non-twisted configuration followed by uniform twists (φ) applied incrementally along the nanotube. The new atomic coordinates are subsequently used as the input to the MD simulator. MD is used to perform relaxation on the twisted CNT until equilibrium is reached and the potential energy of the system converges to a minimum value. By looking at the evolution of the system energy with respect to time, it is found that 40,000 timesteps of 0.5 fs each are enough to reach equilibrium. For each nanotube, the above simulation is conducted at different values of twist/shear strain and it is seen that above a certain value of twist, which is identified as the critical twist for buckling (φ_{cr}), the nanotube collapses into a buckled shape when allowed to relax for a sufficient amount of time (Fig. 4).

Before comparing the results for the critical torques from MD simulations with the nonlocal elasticity shell models, the buckling mode-shapes obtained from the MD simulation are compared with the assumed mode-shapes of the continuum models (e.g. Eq. (5)). For a (8, 0) zigzag nanotube with a length of 10 nm, a radius of 0.31 nm, a shell thickness of 0.08 nm and a Poisson's ratio of 0.2 [29], the buckling wave number calculated from Eq. (9) corresponds to $\lambda = 0.75 \Rightarrow m = 7.4 \,\&\, m/2 = 3.7$. This means that there are 3.7 wavelengths in the longitudinal direction of the buckled nanotube. Fig. 5 shows a MATLAB representation of the assumed buckling mode-shape of the above nanotube based on Eq. (9) and the actual mode-shape obtained from the MD simulations.

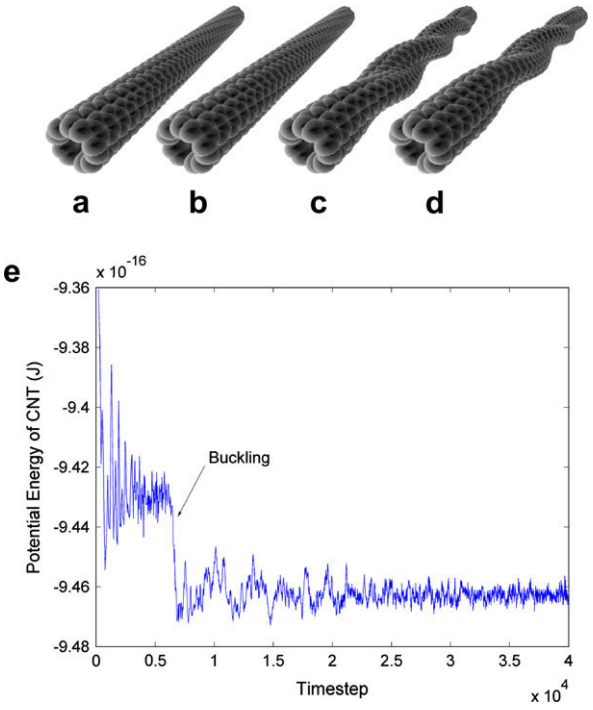

Fig. 4. Relaxation of a (5, 5) armchair nanotube with end twist of 3 radians corresponding to a uniform shear strain of 0.1 for 40,000 timesteps: (a) start of simulation, (b) after relaxation for 6000 timesteps, (c) after relaxation for 6500 timesteps, (d) after relaxation for 40,000 timesteps, and (e) progression of potential energy of the CNT during the 40,000 timesteps of relaxation.

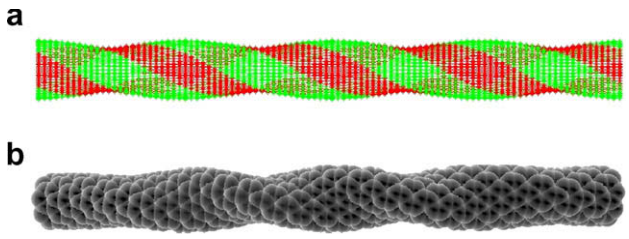

Fig. 5. (a) Representation of predicted buckling mode-shape using MATLAB and (b) actual buckling mode-shape predicted using MD simulations.

Taking into consideration the effects of the fixed boundary conditions at the nanotube ends in the MD model, it is clear from Fig. 5 that buckling mode-shapes of the nonlocal continuum and MD models agree closely. The number of longitudinal waves in the buckled shape corresponding to MD simulations is 3.6 which is very close to the value obtained from the continuum model.

The MD simulator allows the calculation of the potential, kinetic and total energies of the nanotube, its temperature and coordinates of the atoms at each time step. Fig. 6a shows the potential energy (U) progression of a (10, 0) nanotube based on 18 simulations corresponding to different twist angles/shear strains. The slope of the potential energy – twist curve can be related to the torque to obtain a torque-twist relationship. The following basic relationships exist between U, φ, M and torsional stiffness (K):

$$M(\varphi) = \frac{dU(\varphi)}{d\varphi}, \quad K(\varphi) = \frac{d^2U(\varphi)}{d\varphi^2} \tag{16}$$

For a thin cylindrical shell of length L, shell thickness h and shear modulus G the torsional stiffness is defined by $K = 2\pi a^3 Gh/L$. Therefore,

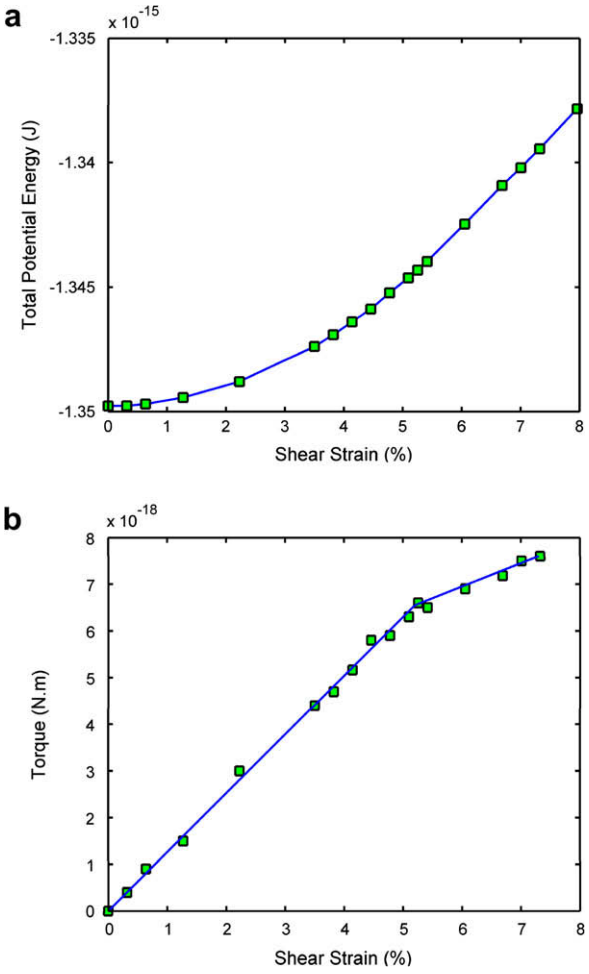

Fig. 6. MD simulation results: (a) variation of potential energy of (8, 0) nanotube with applied shear strain (twist) and (b) stress–strain curve calculated using slope of potential energy curve.

$$G \cdot h = \frac{1}{2\pi a^3} \frac{d^2 U(\varphi)}{d\varphi^2} \tag{17}$$

Eq. (17) can be used to calculate the surface shear modulus ($G \cdot h$) directly from the results of MD simulations and without the need for any assumptions on the value of shell thickness h.

It is important to note that based on the length to diameter aspect ratio ($L/Diam$), a CNT may buckle in the shaft-shape or shell-shape pattern [21]. Previously, the classical formula of Eq. (7) has mostly been used to study the shell-shape buckling of CNTs, which occurs when,

$$\left(\frac{3.9a\sqrt{(1-\upsilon^2)}}{h}\right)^{0.5} \leqslant \frac{L}{Diam} \leqslant \frac{\pi}{4}\left(\frac{1}{3}\left(\frac{D}{Eha^2}\right)^3\right)^{-0.25} \tag{18}$$

A series of torsional buckling simulations are performed on zigzag and armchair nanotubes with different diameters using the MD software. The lengths of the simulated nanotubes are chosen to keep the aspect ratio approximately constant and within the range of Eq. (18). Table 1 shows the critical buckling torque and strain ($\gamma_{cr} = (a/L)\varphi_{cr}$, where γ_{cr} denotes the buckling shear strain).

It is evident from Table 1 that armchair nanotubes generally have a higher torsional stiffness compared to zigzag nanotubes of the same dimensions. However, armchair nanotubes buckle at a lower strain and their critical buckling torque is only slightly higher than a zigzag nanotube of same diameter.

Table 1
Properties and critical torques and twists of: (a) zigzag CNTs and (b) armchair CNTs.

Chiral indices	*Diam* (Å)	Length (Å)	*L*/*Diam*	$G \cdot h$ (GPa nm)	M_{cr} (N m)	φ_{cr} (radians)	γ_{cr}
(a)							
(10, 0)	7.75	122.0	15.7	136.15	6.53E−18	1.65	0.052
(12, 0)	9.30	140.1	15.1	131.19	7.22E−18	1.22	0.041
(14, 0)	10.8	169.8	15.2	127.28	7.67E−18	1.05	0.034
(16, 0)	12.4	184.7	14.9	123.34	8.20E−18	0.85	0.029
(20, 0)	15.5	245.8	15.9	116.00	9.00E−18	0.71	0.022
(b)							
(5, 5)	6.70	98.91	14.8	159.11	5.70E−18	1.50	0.051
(6, 6)	8.05	118.4	14.8	153.17	6.45E−18	1.24	0.042
(8, 8)	10.7	159.9	14.9	148.80	8.01E−18	0.90	0.030
(8, 8)	10.7	243.0	22.7	148.50	8.04E−18	1.38	0.030
(8, 8)	10.7	319.3	29.9	148.60	8.02E−18	1.81	0.030
(10, 10)	13.4	199.0	14.8	145.32	9.66E−18	0.70	0.024
(12, 12)	16.1	238.1	14.8	144.12	1.09E−17	0.55	0.019

The shear modulus values obtained from the present MD simulations are within the range of previously reported experimental and numerical results [5,30]. Using MD simulations, Yakobson et al. [5] reported a value of 363 GPa nm for the in-plane stiffness ($E \cdot h$) and a Poisson's ratio of 0.19 for a (7, 7) armchair CNT. Using these two values the surface shear modulus can be calculated as $G \cdot h = E \cdot h/2(1 + \nu) = 152.5$ GPa nm. Interpolating the surface shear moduli for (6, 6) and (8, 8) armchair nanotubes (Table 1b), we find a value of 151 GPa nm for the surface shear modulus of a (7, 7) CNT. This is almost identical to the value reported by Yakobson et al. The buckling strains obtained in the present study are lower than those reported by Yakobson et al. [5]. This can be due to the use of the AIREBO potential instead of the Tersoff–Brenner potential. The AIREBO potential is an improvement to the Tersoff–Brenner potential. In addition, it is well known that MD simulation results are strain-rate dependent. As the strain rate decreases and the system has more time to relax to an equilibrium state it is seen that properties such as the yield strain decrease [31]. We have performed quasi-static simulations, which consider deformations taking place at infinitely small strain rates. Quasi-static simulations make sure that the deformation of the tube happens simultaneously at all points and there are no localization effects. This contributes to the fact that our buckling strains are smaller than those reported by Yakobson et al. [5].

Hall et al. [30] have performed experimental measurements on the torsional properties of single-wall CNTs. Assuming a shell thickness of 3.4 Å, they calculated an average shear modulus of 0.455 TPa for single wall carbon nanotubes with an average diameter of 1 nm. This corresponds to a surface shear modulus ($G \cdot h$) of 154.7 GPa nm. Table 1b shows that present study yields values of about 150 GPa nm for the surface shear moduli of armchair CNTs with diameters around 1 nm.

4. Calculation of shell thickness and nonlocal constant values

An important issue in the application of the nonlocal elasticity models to CNTs is the determination of the values of the nonlocal elasticity constant e_0, equivalent shear modulus and shell thickness. A direct theoretical relationship between the MD simulations and nonlocal elasticity theory to determine these continuum quantities from the atomistic properties does not exist. However some CNT properties such as the in-plane stiffness ($E \cdot h$), surface shear modulus ($G \cdot h$) and bending rigidity (D) can be defined in terms of measurable characteristics of a CNT without any assumptions for shell thickness. This is seen in Eq. (17) where the surface shear modulus ($G \cdot h$) is calculated directly from the change in the potential energy with applied twist, both of which can be directly ob-

Table 2
Values of shell thickness (h) and nonlocal constant (e_0) obtained from non-linear least-square fitting of MD simulation results with classical shell and nonlocal shell models.

	h (Å)	e_0	Residual norm (nN^2 nm^2)
Armchair			
Classical Timoshenko	0.75		4.11
Nonlocal Timoshenko	0.85	0.85	0.09
Nonlocal Donnell	0.85	0.79	0.1
Zigzag			
Classical Timoshenko	0.81		5.9
Nonlocal Timoshenko	0.86	0.61	0.04
Nonlocal Donnell	0.86	0.57	0.05

tained from MD simulations without the need to assume a value for shell thickness.

One way of addressing the wall-thickness issue is to use values of bending rigidity and in-plane stiffness obtained from MD or *ab initio* simulations together with their classical continuum definitions to calculate the values of shell thickness for use in equivalent continuum models. The aforementioned approach has been used by Kudin et al. where a valued of 0.89 is reported for the CNT shell thickness [32]. Once the shell thickness is calculated, knowing the values of in-plane stiffness, bending rigidity and torsional stiffness, other properties such as the Young/shear modulus can be determined.

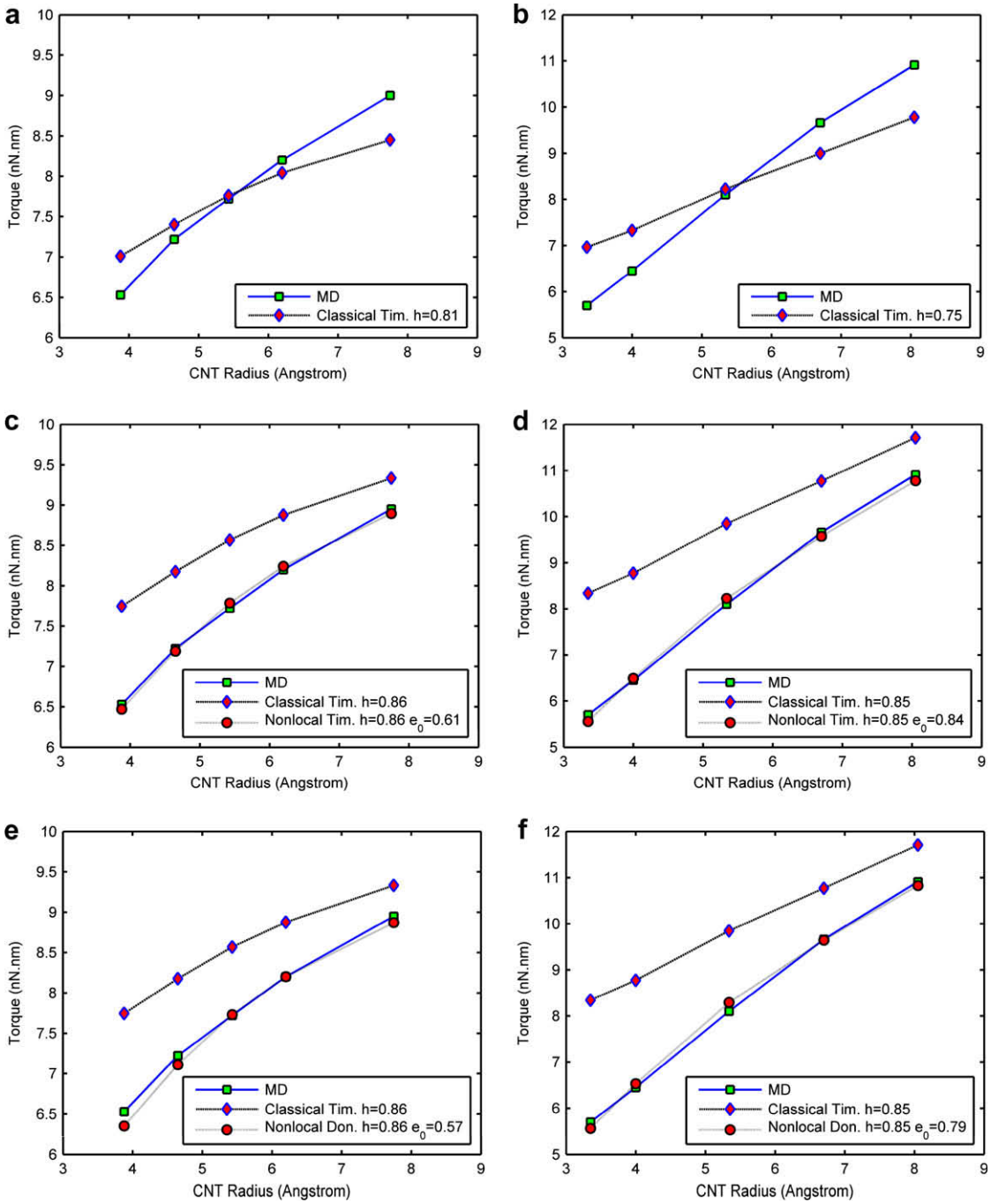

Fig. 7. Comparison of buckling torques from classical shell and nonlocal shell models with MD results for (a), (c), (e) zigzag and (b), (d), (f) armchair CNTs based on properties given in Table 2.

In this paper it is proposed to determine values of shell thickness and the nonlocal constant based on a non-linear least-square fitting by minimizing the Euclidean norm of the difference between the buckling torques obtained directly from the MD simulations and the nonlocal elasticity shell model. This approach will also be used to determine the shell thickness for the classical shell models.

In order to reduce the number of parameters to be determined from the optimization analysis, the surface shear modulus ($G \cdot h$) is obtained directly from the MD torsional simulations and a Poisson's ratio of 0.2 is used based on the existing literature [29]. Therefore, the shell thickness h is considered as the only optimization variable for the classical continuum shell models and both h and e_0 are considered as optimization variables for the nonlocal elasticity based models. Values of h and e_0 obtained from the optimization analysis are shown in Table 2.

The analysis yields a shell thickness of 0.81 and 0.75 Å based on the classical Timoshenko shell model for the zigzag and armchair CNTs respectively. Although these values are close to those previously reported based on theoretical concepts [15], the classical shell model does not show the correct trend of the critical buckling torque with changing diameter (Fig. 7a and b). This fact is also verified by the high residual norm in Table 2. In comparison, the nonlocal elasticity shell models provide a much better fit with the MD results (Fig. 7c–f) over a range of diameters because of the very low residual norms obtained from the analysis as shown in Table 2. The nonlocal Timoshenko shell model predicts a shell thickness of 0.85 and 0.86 Å and a nonlocal constant of 0.85 and 0.61 for armchair and zigzag nanotubes respectively. The nonlocal Donnell shell model predicts a shell thickness of 0.85 and 0.86 Å and a nonlocal constant value of 0.79 and 0.57 for armchair and zigzag nanotubes, respectively.

We note that the values of shell thickness calculated here using the nonlocal shell models are very close to the value of 0.89 Å previously reported by Kudin et al. [30] (only a 5% difference is observed). The difference between the values of e_0 obtained for zigzag and armchair nanotubes may be attributed to the apparent anisotropy of CNT structures introduced due to roll up. An important observation is that changing the aspect ratio of CNTs while keeping within the limits of shell-shape buckling does not affect their torsional properties (rows 3–5 of Table 1b). In other words, if the aspect ratio of the CNT changes within the limits of Eq. (18), the buckling torque, surface shear modulus and the buckling shear strain remain unchanged and the same set of values can be used for the nonlocal constant and shell thickness. Thus, the value of the nonlocal constant is independent of the magnitude of the geometric variables of the system.

5. Concluding remarks

Two nonlocal elasticity based shell models for the torsional buckling of carbon nanotubes are presented by incorporating the nonlocal elasticity based constitutive relations into the classical Timoshenko and Donnell shell models. The non-dimensional buckling torques corresponding to the nonlocal shell models are size-dependent. An important aspect in the application of continuum model to CNTs is the determination of a consistent set of continuum properties for the continuum model. In this regard, a series of nanotubes are analyzed using MD simulations to calculate the critical buckling torque and determine its variation with the tube diameter and chirality (zigzag and armchair). The continuum properties of the CNTs such as the shell thickness and nonlocal elasticity constant are then determined by using non-linear least-square fitting of the MD results with the shell models. This results in consistent values for shell thickness and the nonlocal elasticity constant.

The properties obtained from the least-square fitting shows that for CNTs with small diameters, nonlocal shell models consider the existing size-effects and can accurately model the torsional buckling of CNTs whereas the classical shell models do not. A thickness of 0.85 Å and nonlocal constant (e_0) values of approximately 0.8 and 0.6 for armchair and zigzag nanotubes respectively are recommended for torsional analysis of CNTs by using nonlocal continuum shell models. Furthermore, the present analysis shows that classical shell models overestimate the buckling torques. It is seen that the size-effects in torsional buckling of CNTs become significant when the CNT diameter is small, i.e., for diameters smaller than 1.5 nm there is more than 15% difference between the classical and nonlocal solutions for buckling torque. However changing the length of the CNT within the shell-shape buckling region does not affect the value of buckling torque, and in the case of torsional buckling size-effects are independent of the length or aspect ratio of the CNT.

The present analysis provides consistent values for the shell thickness for two different nanotubes based on the nonlocal elasticity models. This is physically acceptable and furthermore the distinctly different values obtained for the nonlocal elasticity constant of the two types of nanotubes from the current modeling confirms that nonlocal models can effectively quantify the differences in the structural response due to different chiralities.

Acknowledgement

The work presented in this paper was supported by a grant from the Natural Sciences and Engineering Research Council of Canada.

References

[1] S.J. Tans, M.H. Devoret, H. Dai, A. Thess, R.E. Smalley, L.J. Geerligs, et al., Nature 386 (1997) 474–477.
[2] R. Martel, T. Schmidt, H.R. Shea, T. Hertel, P. Avouris, Appl. Phys. Lett. 73 (1998) 2447–2449.
[3] H.W.C. Postma, T. Teepen, Z. Yao, M. Grifoni, C. Dekker, Science 293 (2001) 76–79.
[4] D. Qian, G.J. Wagner, W.K. Liu, M.F. Yu, R.S. Ruoff, Appl. Mech. Rev. 55 (2002) 495.
[5] B. Yakobson, C. Brabec, J. Bernholc, Phys. Rev. Lett. 76 (1996) 2511–2514.
[6] G. Zhou, W. Duan, B. Gu, Chem. Phys. Lett. 333 (2001) 344–349.
[7] M.A.L. Marques, H.E. Troiani, M. Miki-Yoshida, M. Jose-Yacaman, A. Rubio, Nano Lett. 4 (2004) 811–816.
[8] W.A. Curtin, R.E. Miller, Modell. Simul. Mater. Sci. Eng. 11 (2003) 33–68.
[9] G.F. Wang, X.Q. Feng, S.W. Yu, Europhys. Lett. 77 (2007) 44002.
[10] A.C. Eringen, J. Phys. D – Appl. Phys. 10 (1977) 671–678.
[11] J. Peddieson, G.R. Buchanan, R.P. McNitt, Int. J. Eng. Sci. 41 (2003) 305–312.
[12] Y.Q. Zhang, G.R. Liu, J.S. Wang, Phys. Rev. B. 70 (2004) 205430.
[13] Y.Q. Zhang, G.R. Liu, X. Han, Phys. Lett. A 349 (2006) 370–376.
[14] J. Wu, K.C. Hwang, Y. Huang, J. Mech. Phys. Solids 56 (2008) 279–292.
[15] Y. Huang, J. Wu, K.C. Hwang, Phys. Rev. B 74 (2006) 245413.
[16] A.R. Hall, M.R. Falvo, R. Superfine, S. Washburn, Nano Lett. 8 (2008) 3746–3749.
[17] B. Bourlon, D.C. Glattli, C. Miko, L. Forro, A. Bachtold, Nano Lett. 4 (2004) 709–712.
[18] A.R. Hall, M.R. Falvo, R. Superfine, S. Washburn, Nature 2 (2007) 413–416.
[19] X.Y. Wang, X. Wang, J. Reinf. Plast. Compos. 26 (2007) 479–494.
[20] Y.J. Lu, X. Wang, J. Phys. D: Appl. Phys. 39 (2006) 3380–3387.
[21] Q. Wang, S.T. Quek, V.K. Varadan, Phys. Lett. A. 367 (2007) 135–139.
[22] S. Timoshenko, J.M. Gere, Theory of Elastic Stability, McGraw-Hill, New York, USA, 1961.
[23] L. Wang, H. Hu, W. Guo, Nanotechnology 17 (2006) 1408–1425.
[24] Q. Wang, V.K. Varadan, Smart Mater. Struct. 16 (2007) 178–190.
[25] L.H. Donnell, Beams, Plates and Shells, McGraw-Hill, New York, USA, 1976.
[26] NanoRex Inc., 2005, Nanohive-1 v.1.20-b1, www.nanorex.com.
[27] S.J. Stuart, A.B. Tutein, J.A. Harrison, J. Chem. Phys. 112 (2000) 6472–6486.
[28] D.W. Brenner, Phys. Rev. B. 42 (1990) 9458–9471.
[29] J.Z. Liu, Q.S. Zheng, L.F. Wang, Q. Jiang, J. Mech. Phys. Solids 53 (2005) 123–142.
[30] A.R. Hall, L. An, J. Liu, L. Vicci, M.R. Falvo, R. Superfine, et al., Phys. Rev. Lett. 96 (2006) 256102.
[31] T. Dumitrică, B.I. Yakobson, Appl. Phys. Lett. 84 (2004) 2775–2777.
[32] K.N. Kudin, G.E. Scuseria, B.I. Yakobson, Phys. Rev. B. 64 (2001) 235406.